# Performance characteristics for particles of sand FCC and fly ash in a novel hydrocyclone

R.K. Dwari[a], M.N. Biswas[b], B.C. Meikap[a,*]

[a] *Department of Chemical Engineering, National Institute of Technology, Rourkela 769 008, India*
[b] *Department of Chemical Engineering, Indian Institute of Technology, Kharagpur 721 302, India*

**Abstract**

With growing industrialization in power sector and petrochemical industries water has been contaminated with particulates like sand, fly ash and FCC. In the present investigation, a new type of hydrocyclone was designed and fabricated. The system is designed in such a manner that it can operate in a wide range of variables for sand, sand–ash and sand–FCC systems. A detailed study on performance analysis of hydrocyclone, pressure drop, cut size particle diameter and particle characterization has been carried out for the design of the hydrocyclone. A mathematical model for predicting particle separation efficiency and cut size particle diameter has been developed. A correlation has been developed for percentage removal of particles and retention of particles in the hydrocyclone. An experimental finding shows 96% removal efficiency for 175 μm particle with cut size diameter of 75 μm, which can meet the required separation in industrial application.

*Keywords:* Hydrocyclone; Multiphase flow; Separation; Turbulence; Environment; Pollution

## 1. Introduction

Hydrocyclones are widely used to separate particulates from water at high throughput because their advantages like simple structure, low cost, large capacity, and small volume, require little in the way of maintenance and support structure. Hydrocyclones belong to a class of fluid–solid classifying devices that separate dispersed material from a fluid stream. Fluid is subjected to a high-intensity centrifugal force which is created by placing the slurry in a curving path in a cylindrical annulus in a tangential inlet section.

The unit converts the initially linear motion of a fluid into continuously varying angular motion, thereby subjecting the dispersed particulates to centrifugal acceleration and enhancing the rate of settling of particles, according to their differing density, size, and shape.

In the recent past, its applications are widely spread in Environmental Engineering (Chu et al., 1996; Anon, 1997), Petrochemical Engineering (Peachey et al., 1998), Food Engineering (Trim and Marder, 1995; Dickey et al., 1997), Electro-Chemical Engineering (Dhamo, 1994), Bio-engineering (Yuan et al., 1969), Pulping process (Li et al., 1999), and other industrial sectors.

An extensive survey of the literature reveals that fundamental and applied research on the design and performance of hydrocyclone has been continuing for the last five decades. Kelsall (1952) reported the flow pattern and velocity profiles within a hydrocyclone. Bradley and Pulling (1959) studied the flow pattern in the hydraulic cyclone and their interpretation in terms of performance by dye injections into the fluid flowing in the hydrocyclone and have added to detailed knowledge of flow patterns. The results are described and the implications on the theoretical correlation of efficiency are discussed. Such a correlation can never be precise owing to uncertainties in the path followed by an individual particle. Fahlstorm (1963) first investigated the classification of solids with higher concentration (up to 20% by volume). The result was explained in terms of the so-called crowding theory.

Since the time of Fahlstorm (1963), the emphasis of research has been on the development of empirical overall

* Corresponding author. Tel.: +91-661-2476518 ext. 2255; fax: +91-661-2472926.
*E-mail addresses:* bcmeikap@ureach.com, bcmeikap@nitrkl.ac.in (B.C. Meikap).

equations that describe the behavior of large commercial hydrocyclones. The major contribution in this field has been from Lynch and Rao (1966, 1975); Lynch et al. (1974). The use of empirical equation is limited by the fact that the constants and coefficients of the equations need to be evaluated for each and every situation. Larson (1980) reported the characteristics of a new type of hydrocyclone. Luo et. al. (1989) made a comparison of performance of water-sealed and commercial hydrocyclone. Lin (1987) has reported hydrocycloning thickening; dewatering and densification of fine particulates. Chu and Chen (1993) developed a model for the motion of solid particles. Adupeasah et al. (1993) reported a multistage hydrocyclone stirred-tank system for counter current extraction of canola oil. Bendixen and Rickwood (1994) studied the effects of hydrocyclones on the integrity of animal and microbial cell. Dhamo (1994) used an electrochemical hydrocyclone cell for the treatment of dilute solutions which approximate the plug-flow model for electrodeposition kinetics. Trim and Marder (1995) investigated hydrocyclones for concentration of cassava milk. Singh and Eckhoff (1995) suggested hydrocyclone procedure for starch–protein separation in laboratory wet milling. Yuan et al. (1969) made an investigation into the possible use of hydrocyclones for the removal of yeast from beer. Dhamo (1996) investigated the electrochemical oxidation of cyanide in the hydrocyclone cell. Dickey et al. (1997) separated dry-milled corn with hydrocyclone. Klima and Kim (1998) made dense medium separation of heavy metal particles from soil using a wide-angle hydrocyclone. Klima and Kim (1997) used multi-stage wide-angle hydrocyclone circuits for removing fine, high-density particles from a low-density soil matrix. Li et al. (1999) made characterization of hydrocyclone separated eucalypt fiber fraction. Chu et al. worked on numerical simulation of turbulence and structure of turbulence in hydrocyclone.

The structure of hydrocyclone was designed with a series of modifications, and the comprehensive effect of the structural modifications on operation performance. Performance indices of hydrocyclone were investigated experimentally with the orthogonal design method by Chu et. al. (2000). Based on the conventional hydrocyclone, the structural modifications with central insertions named winged core, solid core, and inner diffuser could increase all the separation efficiency, separation sharpness, cut size, capacity and flow split, and decrease the energy loss coefficient. The cut size of the particles is defined as the lowest particle diameter separated with 50% efficiency in the hydrocyclone separator. The effects of geometric and operating parameters and feed characters on the motion of solid particles in hydrocyclones were experimentally investigated by Chu et al. (2002a,b) by using particle dynamic analyzer.

However, despite numerous attempts to produce theoretical prediction of hydrocyclone performance, no fundamental relationship has yet emerged and received general acceptance. Several attempts have been made by Dwari (2003) to predict the cut size that is the size of the smallest particles that can be collected with 50% efficiency.

### *1.1. Analysis and selection of hydrocyclone type*

The requirements of a Hydrocyclone design to have 100% separation efficiency for 70 μm and above silt particles from water with pressure drop not exceeding $0.49 \times 10^5$ Pa and for an inlet particle concentration of 5000 ppm has a few unique features. The design of hydrocyclone must take into consideration very high sharpness of cut (the entire particle above 70 μm must be totally removed), if the cut size is large enough, and energy dissipation must be low and the underflow rate should be as minimum as practicable. In the present study, an attempt has been made to calculate cut size particle diameter and percentage removal efficiency for a new type of cyclone from model as well as experimental data.

## 2. Model formulation for particles

The separation in a hydrocyclone is due to the centrifugal forces generated by the tangential motion of the liquid. When the particle to be separated is of a density different from that of the dispersing liquid they acquire a radial velocity w.r.t. the liquid because of these centrifugal forces. When the particles are of higher densities, this radial velocity is directed outwards and when the centrifugal forces are strong enough the particles reach the cyclone wall on their way from the inlet downwards and are then separated. A particle may not reach the wall

(a) if the radial velocity of the liquid, which is directed inwards, is too large and thus causes it to be entrained towards the centre,
(b) if it enters the cyclone at too great a distance from wall,
(c) the residence time is too short,
(d) on account of turbulence, this causes eddy diffusion of the particles, to the effect that differences in concentration are evened out. The underlying idea for developing the model of the efficiency correlation was that for a certain cyclone there should be a relation between the static pressure drop and the separation achieved when expressed in terms of the 50% separation diameter. This idea was inspired by the fact that the separation as well as the static pressure drop is determined by the centrifugal acceleration field in the cyclone (Heish and Rajamani, 1991).

The model has been developed based on two assumptions made by Rietima (1961) presented below (Scheme 1):

(A) The turbulent eddy diffusion has a negligible effect on the separation.
(B) The Reynolds number as related to the particles separated is so low that Stokes law for the free flow velocity applies.

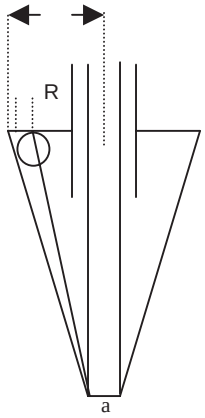


Scheme 1. Schematic separation zone in hydrocyclone

Suppose there is an imaginary screen coaxial with the conical cyclone inlet into two halves of equal cross-sectional area. Under these conditions it is now reasonable to assume that all particles having a diameter equal to the 50% separation efficiency diameter are entering the cyclone through the half of the inner inlet. This leaves the cyclone through the overflow nozzle and those particles with the same diameter entering through the outer half of the inlet leave the cyclone at the apex. A particle of same diameter, which is injected at the center of the inlet, will just be separated. Such a particle will now be considered and followed on its path to the apex.

On injection into the cyclone, its distance from the wall is $= \frac{1}{2}D_i$.

The moment it reaches the apex, its distance from the wall should be reduced to zero.

The radial velocities of the particle then equal $(U - U_p)$.

From Stokes law it follows that for a particle at a radius $r$ in the cyclone

$$U_p = \frac{d_{50}^2 \Delta\rho V_1^2}{18\ \mu_f r}. \tag{1}$$

During its residence time $T$ the particle should cover, in a radial direction, a distance equal to the radius of the inlet center minus the radius of the air core

$$= R - \tfrac{1}{2}D_i - \tfrac{1}{2}a.$$

Therefore

$$\int_0^T (U - U_p)\,\mathrm{d}t = R - \tfrac{1}{2}D_i - \tfrac{1}{2}a = R_1, \tag{2}$$

$$\text{or } \int_0^T U_p\,\mathrm{d}t = \int_0^T U\,\mathrm{d}t - R_1. \tag{3}$$

On the basis of the measurements of Kelsall and Terlinder it may be assumed that both the axial and radial liquid velocities are constant in the separation zone:

$$\int_0^T U_p\,\mathrm{d}t = \int_0^T U\frac{\mathrm{d}L}{W} = \frac{U}{W}L. \tag{4}$$

Eq. (4) can be re-arranged to

$$\frac{d_{50}^2 \Delta\rho}{18\ \mu_f}\int_0^T \frac{V_1^2}{r} = \frac{U}{W}L - R_1 \tag{5}$$

$$\text{or } \frac{d_{50}^2 \Delta\rho}{18\ \mu_f}\int_{R-(1/2)b}^{(1/2)a} \frac{V_1^2}{r}\frac{\mathrm{d}t}{\mathrm{d}r}\,\mathrm{d}r = \frac{U}{W}L - R_1 \tag{6}$$

$$\text{or } \frac{d_{50}^2 \Delta\rho}{18\eta}\int_{R-(1/2)b}^{(1/2)a} \frac{V_1^2}{r}\frac{\mathrm{d}t}{\mathrm{d}r}\,\mathrm{d}r = \frac{U}{W}L - R_1. \tag{7}$$

In the above formula, $\mathrm{d}t/\mathrm{d}r$ expresses the reciprocal radial velocity of the particle. When it is assumed that the axial velocity of the particle under consideration is equal to that of the liquid and is therefore constant it follows that on an average the radial velocity of the particle must also be constant otherwise, the particle would leave the separation zone very close to the wall and then it would not be separated.

On an average $\mathrm{d}r/\mathrm{d}t \approx (W/L)R_1$ and

$$\frac{\mathrm{d}t}{\mathrm{d}r} = \frac{L}{W}\frac{1}{R_1}. \tag{8}$$

For a liquid cyclone operating with a gas core, the static pressure drop is equal to the centrifugal head:

$$(\Delta P)_s = \int_{R-(1/2)b}^{(1/2)a} \frac{\rho V_1^2}{r}\,\mathrm{d}r. \tag{9}$$

The separation formula can now be elaborated to

$$\frac{d_{50}^2 \Delta\rho}{18\ \mu_f}\frac{L}{W}\frac{1}{R_1}\frac{(\Delta P)_s}{\rho} = \frac{U}{W}L - R_1, \tag{10}$$

$$\rightarrow \frac{d_{50}^2 \Delta\rho}{18\ \mu_f}\frac{1}{R_1}\frac{(\Delta P)_s}{\rho} = \frac{W}{L}\left(\frac{U}{W}L - R_1\right) \tag{11}$$

$$\rightarrow \frac{d_{50}^2 \Delta\rho}{18\mu_f}\frac{1}{R_1}\frac{(\Delta P)_s}{\rho} = \frac{W}{L}\frac{U}{W}L - WR_1/L_1 \tag{12}$$

$$\rightarrow \frac{d_{50}^2 \Delta\rho}{18\mu_f}\frac{1}{R_1}\frac{(\Delta P)_s}{\rho} = U - \frac{WR_1}{L}. \tag{13}$$

However, the above model did not take into account radial velocity components in terms of hydrocyclone pertinent characteristics. An attempt has been made to modify the model based on the above criteria.

Radial velocity of liquid

$$U = \frac{Q}{2\pi rL}, \tag{14}$$

when $r$ is at any radius.

Relation between axial velocity and inlet velocity is assumed as $W = C_1 V$.

Putting the value of $U$ and $W$ in the above equation we obtain

$$\frac{d_{50}^2\Delta\rho}{18\ \mu_f}\ \frac{1}{R_1}\ \frac{(\Delta P)_s}{\rho} = \frac{Q}{2\pi rL} - \frac{C_1 V R_1}{L}. \tag{15}$$

The particle can be separated at 50% efficiency when it is at a distance equal to half the radius of hydrocyclone that is $r = R/2$.

Putting the value in the above equation we obtain

$$\frac{d_{50}^2\Delta\rho}{18\ \mu_f}\ \frac{1}{R_1}\ \frac{(\Delta P)_s}{\rho} = \frac{Q}{2\pi(R/2)L} - \frac{C_1 V R_1}{L} \tag{16}$$

$$\rightarrow \frac{d_{50}^2\Delta\rho}{18\mu_f}\ \frac{1}{R_1}\ \frac{(\Delta P)_s}{\rho} = \frac{Q}{\pi RL} - \frac{C_1 V R_1}{L}. \tag{17}$$

Rearranging the above equation for $d_{50}$, we obtain

$$d_{50} = \sqrt{\left(\frac{Q}{\pi RL} - \frac{C_1 V R_1}{L}\right)\frac{18\mu_f R_1 \rho}{\Delta\rho\Delta P_s}}. \tag{18}$$

Eq. (18) is used to calculate $d_{50}$, the cut size for the present system hydrocyclone.

## 3. Experimental setup and technique

The experimental set up as shown in Fig. 1 has been used for the studies of performance characteristic of hydrocyclone consisting of a vertical cylindrical portion and conical portion. The experimental setup mainly comprises a hydrocyclone, centrifugal pump and collection and supply tank. The hydrocyclone is of mild steel of cylindro-conical structure having a cyclone diameter of 0.24 m. The length of the cylindrical portion is 0.3 m and that of the conical portion is 0.74 m. The cylindrical part is closed on top by a flat head through which the liquid overflow pipe known as a vortex finder having a diameter of 0.15 m protrudes some distance into the cyclone body. At the bottom of the conical section, a split chamber is attached through which an adjustable apex pipe having a diameter of 0.04 m has been fitted through which coarser particles will move. The apex pipe can be raised or lowered to obtain a suitable air core for getting maximum separation. Densely concentrated coarser particles can be separated from the split chamber. The slurry is injected tangentially by an inlet pipe of diameter 0.04 m fitted tangentially to the cylindrical portion of hydrocyclone.

A tank having a storage capacity of 1000 l has been placed as shown in the figure ($T_1$). The slurry is pumped to the cyclone by a 10 H.P centrifugal pump ($P_1$). There is a gate valve ($V_1$) between the tank and the centrifugal pump. The volumetric flow rate of feed slurry can be maintained by regulating the flow through a gate valve ($V_1$) between tank ($T_1$) and centrifugal pump ($P_1$) and by regulating the gate valve ($V_2$) through the bypass line. The flow through apex and split chamber can be controlled by valve ($V_3$) and valve ($V_4$).

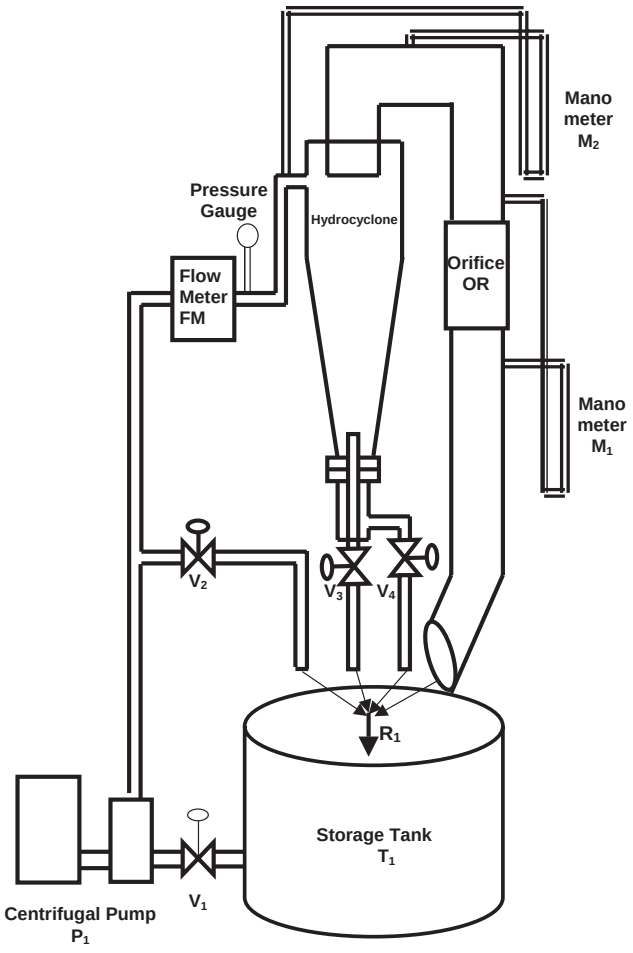


Fig. 1. Experimental setup.

The suction pipe fitted to the centrifugal pump has a diameter 0.1016 m and that of delivery pipe 0.0762 m. The pipe is reduced to 0.04 m just before injecting the slurry to the hydrocyclone. The volumetric flow rate through the pipe can be measured by a flow meter (FM) fitted in the delivery pipe. A pressure gauge (PG) between FM and the inlet section of hydrocyclone measures the inlet fluid pressure. An orifice (OR) is fitted in the overflow stream and a manometer ($M_1$) filled with $CCl_4$ is provided to measure the pressure drop across the orifice. Through proper calibrations, this pressure drop can be used to measure the flow rate in the overflow. Calibration of flow through the orifice is carried out closing the apex valve ($V_3$). Inlet flow rates were adjusted by valve $V_1$ and $V_2$ of the suction and bypass lines. The pressure drop was measured by carbon tetrachloride manometer ($M_1$). The flow rate was calibrated in terms of pressure drop across the orifice.

A mercury manometer ($M_2$) was provided to measure the pressure drop across the hydrocyclone.

The flow from overflow, apex and split were recycled to the tank, so that the slurry concentration in the tank was maintained a constant. The test points were provided at inlet and overflow streams for sample collection.

Sand, fly ash, and FCC were used for the experimental performance study of the hydrocyclone. Experiments were conducted for sand-water slurry of 5000 ppm prepared in a tank ($T_1$) by mixing 2.5 kg of sand with 500 l of water. The suction valve was made to open to create positive suction head at the centrifugal pump. Then the centrifugal pump was switched on, which injected the slurry at high velocity to the hydrocyclone. At a low inlet pressure of around 17.5 kN/m$^2$, proper vortex did not develop. By increasing the velocity of flow, an inlet pressure around 20 kN/m$^2$ vortexes was created and flow through overflow pipe began. Flow from vortex, underflow, apex, and bypass line recycled (R1) to the tank, made high turbulence within the tank which inturn maintained the slurry at uniform concentration. Then the flow rate was maintained at 27.6 kN/m$^2$. When the flow attained the steady state, slurry samples were collected from the inlet, vortex, apex and split chamber and the following measurements were taken for the inlet flow rate, inlet flow pressure, pressure head in $CCl_4$ manometer and in mercury manometer to find out the pressure drop across the hydrocyclone. For each inlet flow, four samples were collected at the inlet, overflow, and underflow and split chamber for particle size analysis.

The similar process was repeated at 41.4, 55.2 and 69.0 kN/m$^2$ inlet pressures. In all the case samples were collected and readings were noted. Similarly for sand and fly-ash-water system, slurry of sand and fly ash of 5000 ppm was prepared by mixing 1.25 kg sand and 1.25 kg fly ash with 500 l of water. Then the experiment was repeated as described above. The same procedure was applied for the slurry of sand–FCC–water system, where a slurry of FCC of 5000 ppm was prepared by mixing 1.25 Kg sand and 1.25 Kg fly ash with 500 l of water at different experimental conditions as described above. The experimental conditions are presented in Table 1.

The particle size distributions were measured by a method as reported by Meikap et al. (2002). The Malvern particle size analyzer equipment analyzed the particle size of each sample. A typical plot of particles size distribution is shown in Fig. 2a. By knowing the particle size at inlet and overflow, the efficiency of separation of each particle by hydrocyclone can be calculated by using the following equation for efficiency of separation of particle:

$$\eta = \frac{\text{Wt\% of particle at inlet} - \text{Wt\% of particle at overflow}}{\text{Wt\% of particle at inlet}} \times 100. \quad (19)$$

Table 1
Experimental conditions in the hydrocyclone

| Variables | Range of variables |
|---|---|
| Inlet pressure of slurry, $P$ (kN/m$^2$) | 27.4, 41.4, 55.2 and 69.0 |
| Volumetric flow rate, $Q \times 10^3$(m$^3$/s) | 4.5, 6.0, 7.5 and 8.3 |
| Difference in pressure head $\Delta H$ for sand (kN/m$^2$) | 2.63, 4.27, 5.26 and 6.58 |
| Difference in pressure head $\Delta H$ for sand and fly ash (kN/m$^2$) | 2.96, 3.95, 5.59 and 6.90 |
| Difference in pressure head $\Delta H$ for sand and FCC (kN/m$^2$) | 2.96, 3.95, 4.93 and 8.55 |
| Average particle diameter for sand (μm) | 90.0–93.3 |
| Average particle diameter for sand and fly ash (μm) | 20.07–20.73 |
| Average particle diameter for sand and FCC (μm) | 76.88–76.92 |
| Temperature (°C) | 27–30 |

## 4. Results and discussions

Experiments have been conducted for different concentrations of sand, fly ash and FCC particles to characterize the performance of a hydrocyclone. The materials have been chosen at its present importance; like from the thermal power plants and petrochemical industries. The polluted water can be treated for removal of these types of materials by using a hydrocyclone. Experiments were conducted at inlet flow pressures of 27.6, 41.4, 55.2 and 69.0 kN/m$^2$. Different slurries made of sand–water, sand–fly-ash–water, and sand–FCC–water were used for experimental investigation. The slurry volumetric flow rate used for experimental studies was in the range of $4.5 \times 10^{-3}$–$8.3 \times 10^{-3}$ m$^3$/s ($4.5\times10^{-3}$, $6.0\times10^{-3}$, $7.5\times10^{-3}$ and $8.3\times10^{-3}$ m$^3$/s). The experimental data with various slurry flow rates, inlet slurry flow pressures and pressure drop across the hydro-cyclone have been measured.

The particle size distribution of samples collected at inlet, overflow, split chamber and apex were measured using a Malvern-3601 particle size analyzer using $Na_4P_2O_7$ (anhydrous)[LOBA Chemie] as dispersant in a concentration of 1.0864 kg/m$^3$ and the results of the particle size distribution are presented in Fig. 2a for various systems. The efficiency of the separation of particles was calculated by knowing the particle size% in bands of inlet and overflow samples using Eq. (19) mentioned in Section 3. The efficiency of separation of particles was calculated for slurry velocities of 3.56, 4.77, 6.0 and 6.62 m/s. The trend of the variation of percentage removal particles have been plotted in Figs. 2–14 at various inlet velocities and operating variables for the 0.24 m hydrocyclone.

### 4.1. Effect of particle diameter on separation efficiency

The percentage separation of sand, sand and fly ash, sand and FCC has been plotted against particle diameter

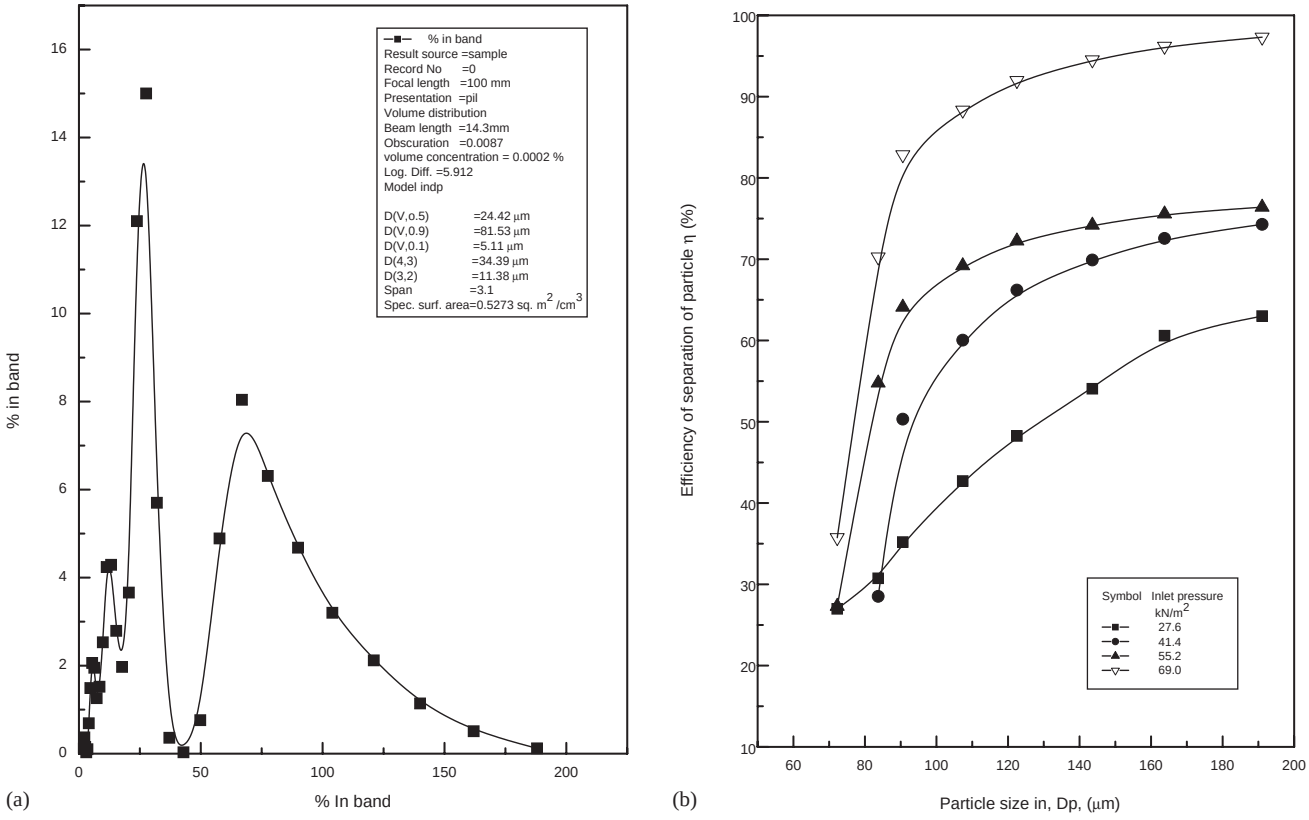


Fig. 2. (a) Malvern particle size analysis for sand inlet sample at 27.6 kN/m$^2$ inlet slurry pressure. (b) Effect of particle diameter on efficiency of separation of sand.

in Figs. 2–4. From these plots it can be seen that with increasing particle size, the efficiency of separation increases almost exponentially at inlet pressures of 69.0, 55.2 and 41.4 kN/m$^2$. It can also be seen from Fig. 2 that at low pressure i.e. 27.6 kN/m$^2$, the cut size, the 50% efficiency of separation is 157 μm; at 41.4 kN/m$^2$, the 50% efficiency of separation of particles is 91 μm; at 55.2 kN/m$^2$, the 50% efficiency of separation of particles is 77.5 μm and at 69.1 kN/m$^2$, the 50% efficiency of separation of particles is 71.5 μm. It is interesting to note that at 69.1 kN/m$^2$, the efficiency of separation is almost 100% for particles above 188 μm. It is quite obvious that with increasing pressure of the cyclonic motion, the larger particles are removed easily. So with increase in particle size, at a particular inlet pressure, the efficiency of separation increases. As shown in the figure with increasing inlet pressure the efficiency of separation of each particle size range also increases. At high inlet pressure, the particles separate more efficiently.

Fig. 3 represents the effect of particle size on the efficiency of separation of sand and fly ash of sand–fly-ash–water system. It can be seen from this figure that with increasing particle size, the efficiency of separation is increased at all inlet pressures and at low pressures 27.6 kN/m$^2$, the cut size, the 50% efficiency of separation of particles is 141 μm, at 41.4 kN/m$^2$, the 50% efficiency of separation of particles is 66 μm; at 55.2 kN/m$^2$, the 50% efficiency of separation of particles is 60 μm and at 66.9 kN/m$^2$, the 50% efficiency of separation of particles is 50 μm. This figure shows that at high three-inlet pressures the efficiency of separation of particles in the range of 188 μm is 100%. Up to 75 μm, the size particle separation efficiency increases rapidly and that of particles between 75 and 140 μm, though the efficiency increases, it is not as rapid as before. This may be due to the presence of a heterogeneous mixture of suspended particles of sand and fly ash in the slurry. It is also seen from this figure that there is a rapid increase in separation efficiency for particles more than 140 μm size with an increase in particle diameter.

Similar trend have also been observed for other sets of experimental conditions shown in Fig. 4. It can be seen from this figure that at inlet slurry pressures 27.6, 41.4, 55.2 and 69.0 kN/m$^2$, the cut size, 50% efficiency of separation of particles are 198 μm, 176 μm, 138 μm and 136 μm, respectively. The figure shows that the efficiency of separation almost increases linearly with increase in particle size.

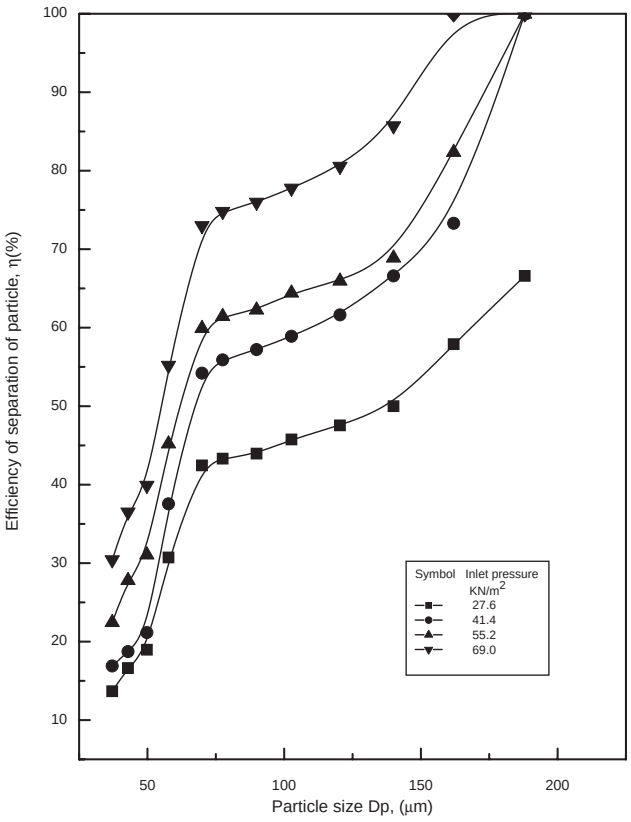


Fig. 3. Effect of particle size on efficiency of separation of sand and fly ash.

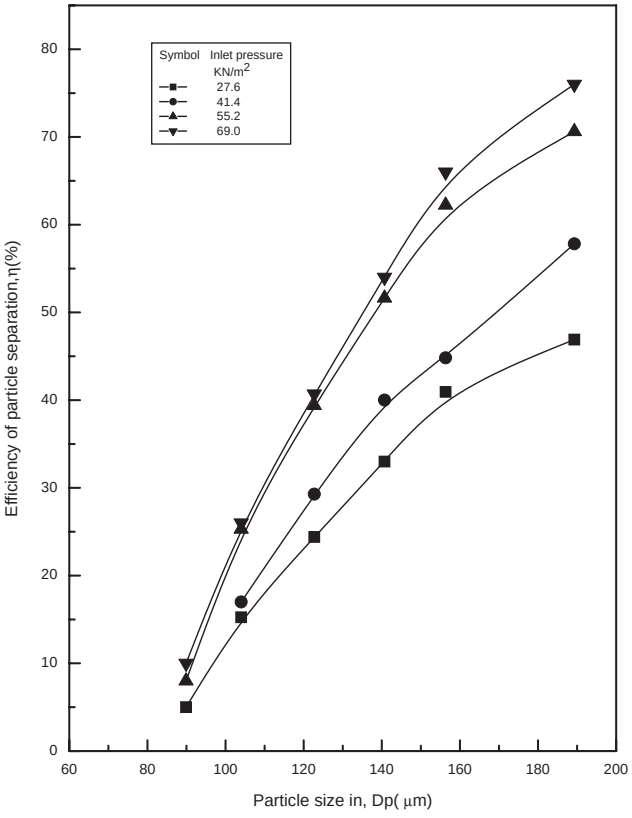


Fig. 4. Effect of particle size on efficiency of separation of sand and FCC mixture.

### *4.2. Effect of velocity of flow on the efficiency of separation of particles*

The effect of slurry velocity, V, on the percentage separation of sand, sand-fly ash and sand-FCC has been presented in Figs. 5–7. It can be seen from these figures that, with increase in velocity the efficiency of separation increases, and this may be due to the increasing swirling in the hydrocyclone, which is also confirmed by the other researchers cited in the literature. An almost similar trend has been observed for other sets of experimental conditions, that the largest particle has high efficiency of separation, and efficiency increases with increase in the velocity of flow.

### *4.3. Effect of pressure drop on efficiency of separation of particles*

The effect of pressure drop, $\Delta P$, on percentage removal of particles for sand, sand–fly ash and sand–FCC has been presented in Figs. 8–10. The variations have been plotted for different particle diameters. It can be seen from these figures that with an increase in pressure drop the separation efficiency increases. Fig. 8 shows that 75 μm sand particles have low percentage removal (35%) up to 430 $N/m^2$. After a certain pressure drop of 450 $N/m^2$ the increase in pressure drop particle separation increases steadily. It can also been found that for 89.9 μm bigger particles have almost the same efficiency of separation. At any particular pressure drop larger particles have high separation efficiency than smaller particles. Fig. 9 also shows similar separation characteristics for all range of particles of sand–fly ash. Fig. 10 shows a typical plot of variation of particle-separation efficiency with pressure drop for sand–FCC. It can be seen from this plot that with increase in pressure-drop percentage, removal of particles increases rapidly up to 500 $N/m^2$ pressure drops, after that separation percentage is almost constant for each particle. The reason may be because two opposite facts act on the particles. As increase in pressure drop is related to high velocity, which has already been discussed; on the other hand due to higher pressure drop the eddies formed around the vortex lead to lower efficiency of separation. As a result, beyond a pressure drop of 500 $N/m^2$ the increase in the efficiency of separation of the particles is very slow.

### *4.4. Effect of velocity on cut size particle diameter*

The separation formulae derived by Rietima (1961) has been modified for application to the present system discussed

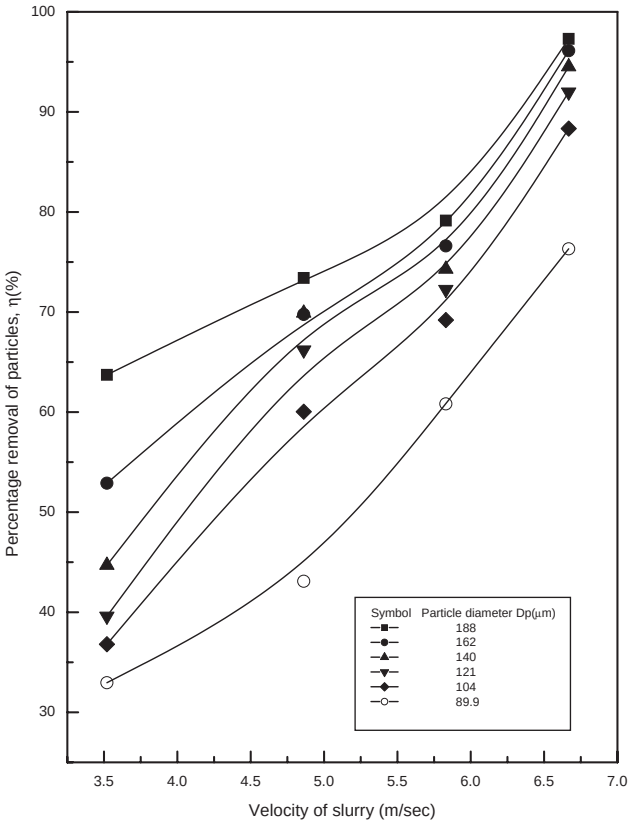


Fig. 5. Effect of velocity of flow on efficiency of separation of particles of sand.

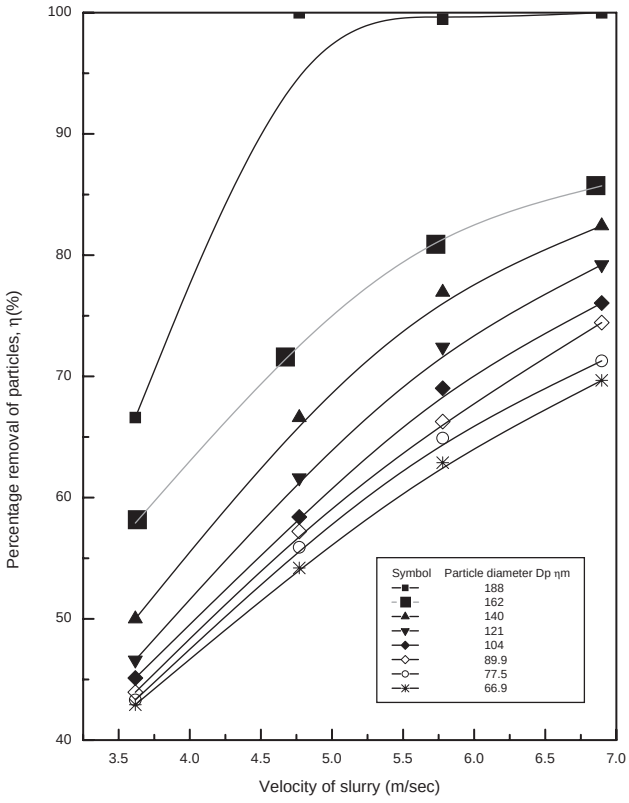


Fig. 6. Effect of velocity of flow on efficiency of separation of particles of sand and fly ash.

earlier to calculate $d_{50}$, cut size particle diameter that is, 50% efficiency of separation of particle expressed by Eq. (2)

$$d_{50} = \sqrt{\left(\frac{Q}{\pi RL} - \frac{C_1 V R_1}{L}\right) \frac{18\ \mu_f R_1 \rho}{\Delta\rho \Delta P_s}}. \tag{20}$$

For different inlet flow velocity $V$ of slurry and pressure drop $\Delta P$ across the hydrocyclone, $d_{50}$ values were calculated for sand, sand–fly ash and sand–FCC system. The $d_{50}$ value was also calculated using Dahlstroms (1951) correlation given below and compared with the experimental findings of the present system:

$$d_{50} = \frac{2248.5(D_i D_o)^{0.68}}{Q^{0.53}} \times \left[\frac{1.73}{\rho_s - \rho}\right]^{0.5}. \tag{21}$$

The predicted values and $d_{50}$ data obtained from experimental results have been calculated for sand, sand–ash, and sand–FCC, respectively. The effect of slurry velocity on cut size particle diameter, $d_{50}$ has been presented in Figs. 11–13 for sand, sand–ash, and sand–FCC system. It can be seen from these figures that with increase in velocity the cut size decreases. It is interesting to note that at low slurry velocity range cut size particle diameter predicted from the model equations developed fits very well than that calculated from Dahlstroms (1951) correlation. However, at high slurry velocity the cut size particle diameter predicted by the model is higher than that of both the experimental values and calculated from Dahlstroms (1951). It can also be seen from these figures that experimental cut size diameter is less than predicted from the model but greater than the cut size diameter calculated from Dahlstroms correlation.

### 4.5. Effect of slurry velocity on pressure drop

The pressure drop data for sand, sand–ash and sand–FCC have been plotted against velocity as shown in Fig. 14. It can be seen from this figure that for all types of material the pressure drops of the system increases with increase in slurry velocity. It has been observed that the pressure drop for sand–FCC is higher than that of sand and sand–fly ash system. It is quite obvious that with increase in velocity, pressure drop increases due to frictional losses. The frictional and eddy losses may be more prominent for sand–FCC than the sand and sand–fly ash system, that is why the pressure-drop increase in the case of sand–FCC is more after a 6.0 m/s velocity.

## 5. Development of correlation

As the motion of particle and fluid inside a hydrocyclone is very complex, the possibility of using any one of the proposed models or empirical correlations, with a degree of ac-

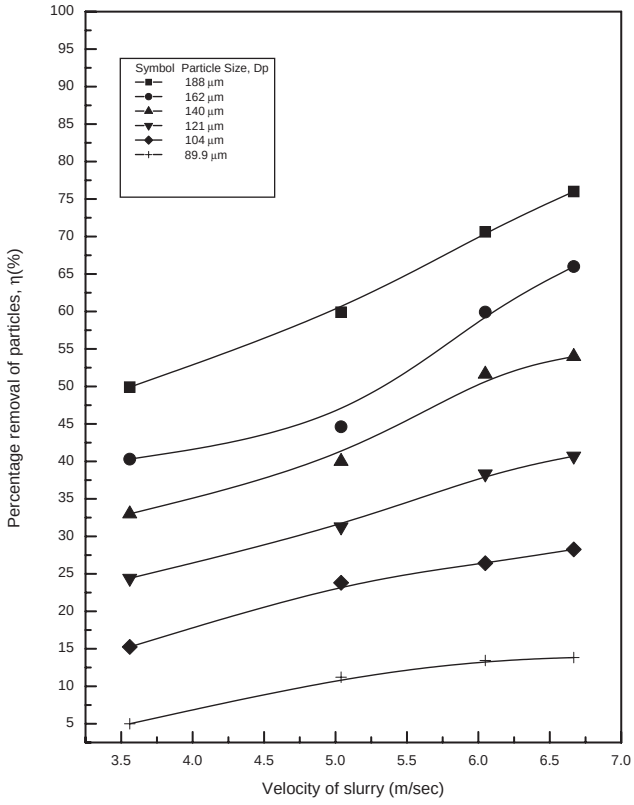


Fig. 7. Effect of velocity of flow on efficiency of separation of particles for sand and FCC.

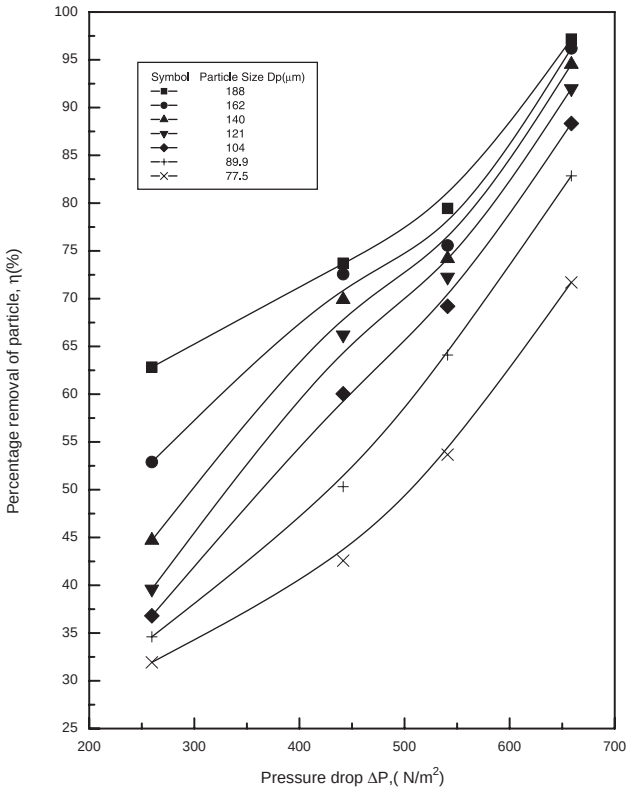


Fig. 8. Effect of pressure drop on efficiency of separation of particles for sand.

curacy, was therefore found difficult for the present system. Hence, the experimental separation efficiency has been analyzed on the basis of dimensionless analysis to predict the removal efficiency of the hydrocyclone.

Conceivable variables on which the efficiency of separation of particles in the hydrocyclone may depend are: flow properties fluid velocity V; physical properties namely diameter of suspended particle $d$, density of suspended particle $\rho_s$, density of fluid $\rho$, viscosity of fluid $\mu_f$; geometric properties: hydrocyclone diameter $D_c$, diameter of eductor $D_e$, and inlet diameter $D_i = f(D_c, D_u)$. The large numbers of possible variables on which the efficiency of separation depend have been reduced to a pertinent few, since many of these variables are interrelated or are maintained constant. A theoretical relation exists between the efficiency of separation $\eta$, and the physical characteristic, and the fluid variable of the system. Then $\eta$ may be written in the following form:

$$\eta = f(\rho_s, \mu_f, d, D_i, V, \rho). \tag{22}$$

The dimensional analysis carried out as above indicates that the efficiency of separation may be simplified to the equation

$$\eta = f_2 \left(\frac{\mu}{\rho_s V D_i}\right)^a \left(\frac{d}{D_i}\right)^b \left(\frac{\rho}{\rho_s}\right)^c. \tag{23}$$

Or retention of particles in water;

$$\mathrm{RP} = 1 - \eta = 1.0 - Z \left(\frac{\mu}{\rho_s V D_i}\right)^a \left(\frac{d}{D_i}\right)^b \left(\frac{\rho}{\rho_s}\right)^c. \tag{24}$$

Therefore Eq. (24) gives an expression for the retention of particles in the hydrocyclone are a measure of efficiency of separation.

The dimensionless analysis presented earlier indicates that the percentage separation efficiency of particles presented in Eq. (23), may be simplified to

$$\eta = S \left(\frac{\mu}{\rho_s V D_i}\right)^a \left(\frac{d}{D_i}\right)^b \left(\frac{\rho}{\rho_s}\right)^c, \tag{25}$$

as the values of other parameters remained constant or their variations were negligible.

In order to establish the functional relationship between percentage separation efficiency of particles, $\eta$ and the various dimensionless groups in Eq. (23), multiple linear regression analysis has been used to evaluate the constants and coefficients of the equation.

It can be seen that the following equation, which yields the minimum percentage error and minimum standard deviation of percentage error, presents the best possible correlation among the family of equations. So the following form of equation with the minimum percentage deviation of error presents the best possible correlation among the family of

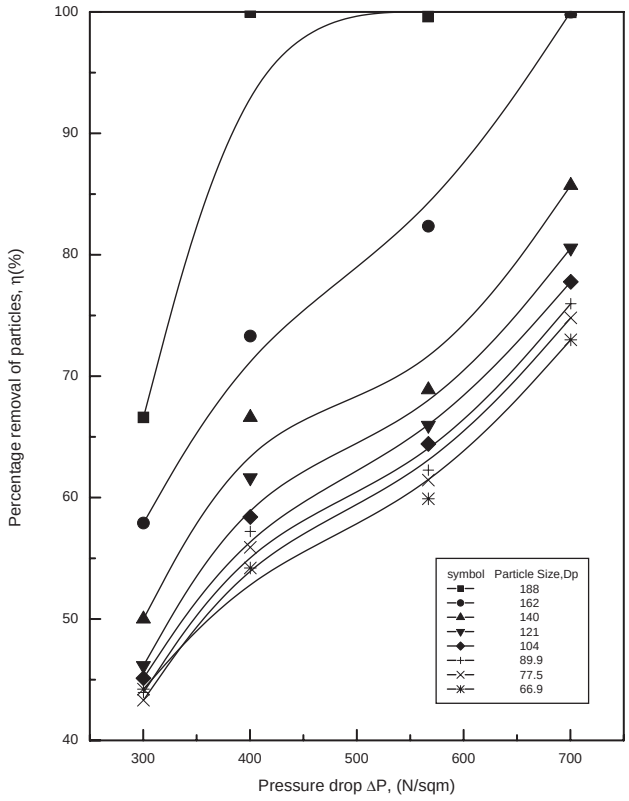


Fig. 9. Effect of pressure drop on efficiency of separation of particles for sand and fly ash.

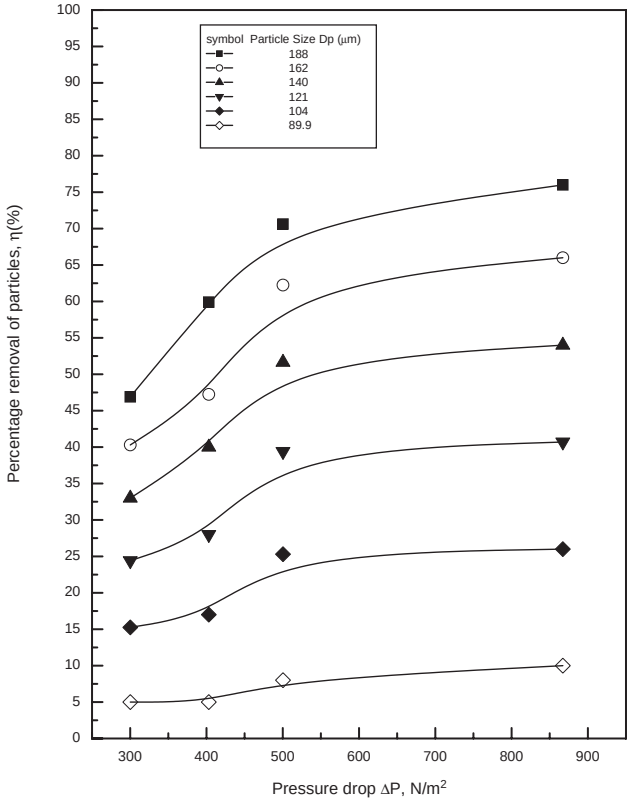


Fig. 10. Effect of pressure drop on efficiency of separation of particle for sand and FCC.

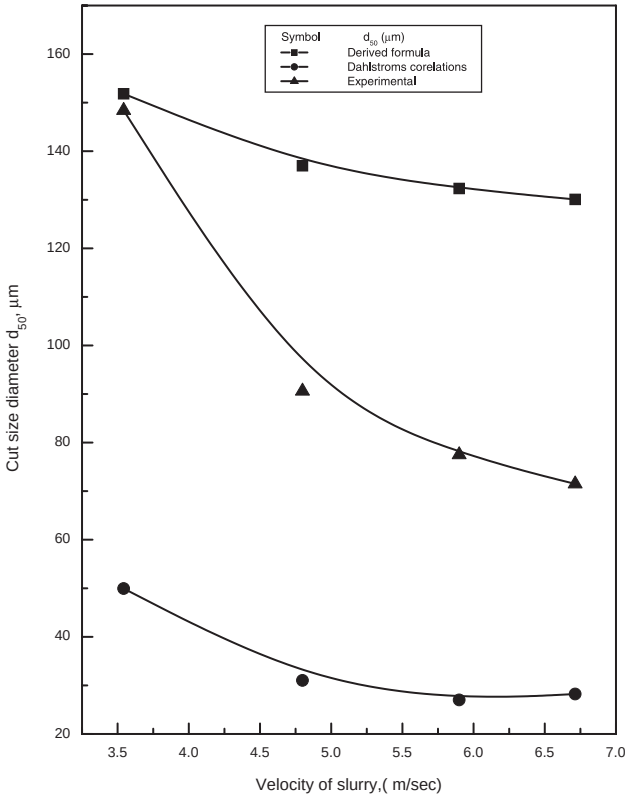


Fig. 11. Effect of velocity on cut size, $d_{50}$ for sand.

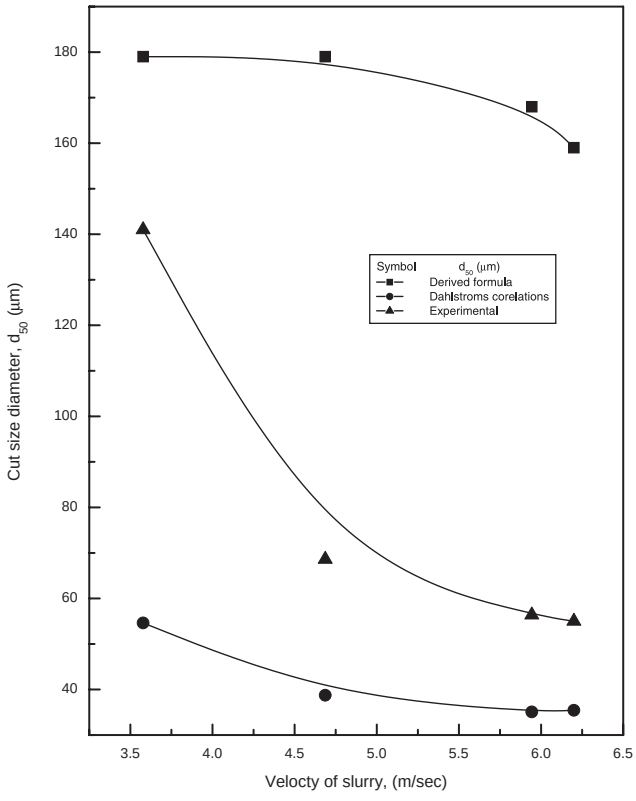


Fig. 12. Effect of velocity on cut size, $d_{50}$ for sand and fly ash.

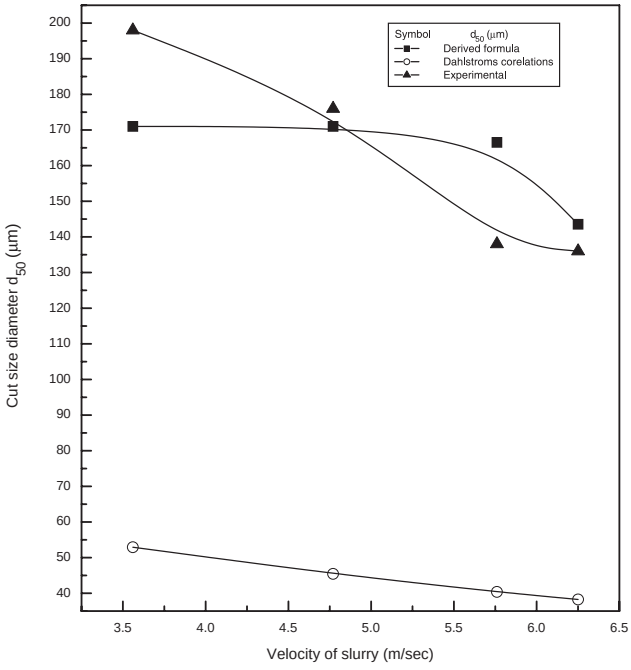


Fig. 13. Effect of velocity on cut size, $d_{50}$ for sand and FCC.

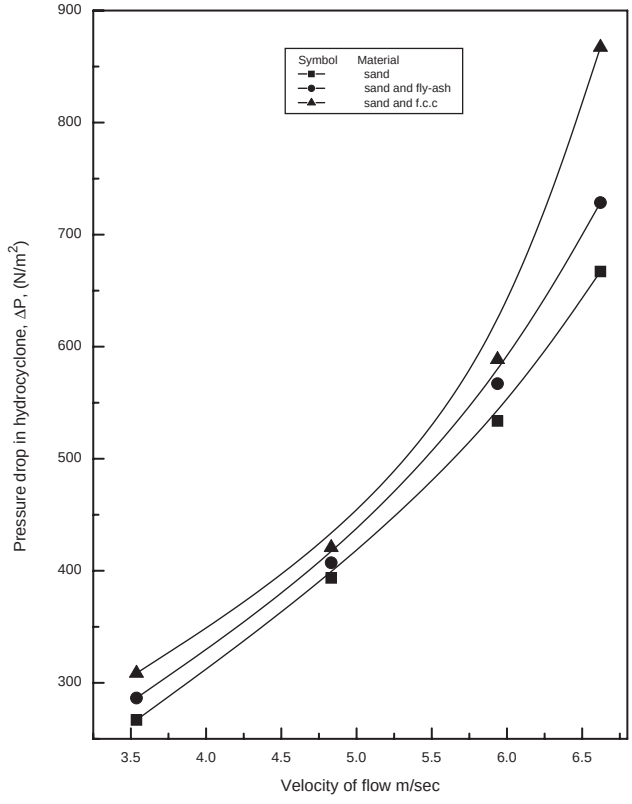


Fig. 14. Effect of velocity of flow on pressure drop in hydrocyclone.

equations presented here;

$$\eta = 0.1 \times 10^{-02} \left(\frac{\mu}{\rho_s V D_i}\right)^{-0.82} \left(\frac{d}{D_i}\right)^{0.63} \left(\frac{\rho}{\rho_s}\right)^{0.82}. \quad (26)$$

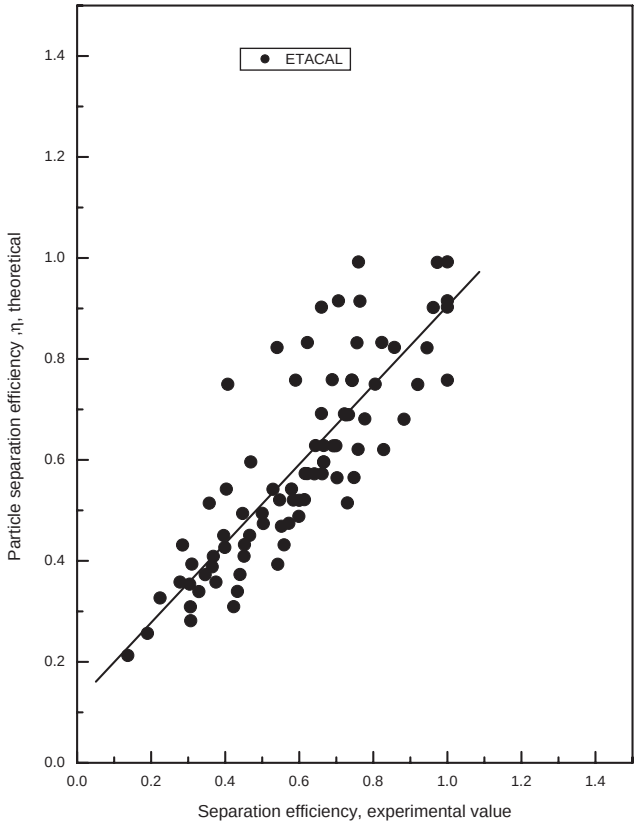


Fig. 15. Comparison of theoretical and experimental values of particle separation efficiency.

Eq. (26) describes the percentage separation efficiency *of* particles, $\eta$ in the hydrocyclone, which is an important parameter for assessing the performance of the hydrocyclone.

The form of equation can be rearranged to

$$\mathrm{RP} = 1 - \eta = 1.0 - 0.1 \times 10^{-02} \left(\frac{\mu}{\rho_s V D_i}\right)^{-0.82} \times \left(\frac{d}{D_i}\right)^{0.63} \left(\frac{\rho}{\rho_s}\right)^{0.82}. \quad (27)$$

Eq. (26) actually describes the particle penetration within the hydrocyclone, which is an important parameter for assessing the performance of the hydrocyclone.

The values of the parameter can be expressed as

$$\mathrm{RP} = 1 - \eta = 1.0 - 0.1 \times 10^{-02} \left(\frac{\mu}{\rho_s V D_i}\right)^{-0.82} \times \left(\frac{d}{D_i}\right)^{0.63} \left(\frac{\rho}{\rho_s}\right)^{0.82}. \quad (28)$$

This parameter was calculated for the experimental data. The values of percentage separation efficiency of particles, $\eta$ predicted by Eq. (26) have been plotted against the experimental values of percentage separation efficiency of particles, $\eta$ in Fig. 15. The percentage deviation between the experimental data and those predicted by Eq. (26) has been

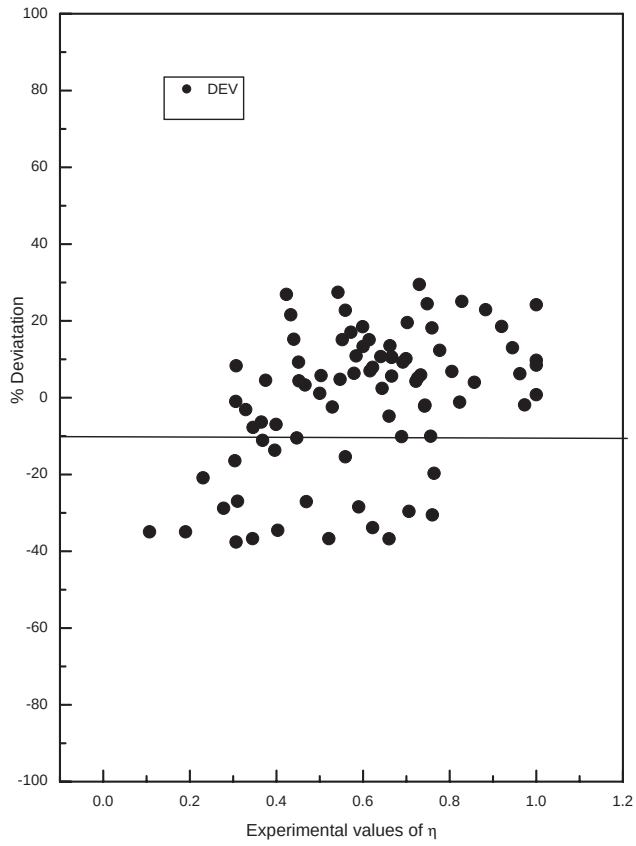


Fig. 16. Deviation between experimental values and calculated values of separation efficiency.

plotted in Fig. 16. It is seen from this figure that the percentage deviation is quite low (within ±22.5%).

Furthermore to test the acceptability of the correlation various statistical tests have been carried out.

### 5.1. Statistical analysis of the correlation

The following statistical parameters have been calculated to test the significance of the correlation.

Sum of the squares of deviation removed by regression.

$$\sum{}' c^2 = 9.948918 \tag{29}$$

$$\text{Sum of the squares of deviation} : \sum{}' y^2 = 13.297. \tag{30}$$

Residual sum of squares of deviation

$$\sum{}' P_1^2 = \sum{}' y^2 - \sum{}' c^2 = 13.297 - 9.948918 = 3.348082. \tag{31}$$

$$\text{Correlation coefficient } r = \sqrt{\frac{\sum C^2}{\sum Y^2}} = 0.86499. \tag{32}$$

$$\text{Variance of estimate } s^2(Y) = \sum{}' P_1^2/(N-K-1) = 0.042386. \tag{33}$$

The diagonal Gaussian multipliers for the correlation are

$$C_{11} = 0.201369, \tag{34}$$

$$C_{22} = 0.061303, \tag{35}$$

$$C_{33} = 1.029758. \tag{36}$$

Degree of freedom = 83

Variance of regression coefficients

$$S^2(b_1) = s^2(y) \times C_{11} = 8.535 \times 10^{-3}, \tag{37}$$

$$S^2(b_2) = s^2(y) \times C_{22} = 2.598389 \times 10^{-3}, \tag{38}$$

$$S^2(b_3) = s^2(y) \times C_{33} = 0.0436473. \tag{39}$$

The $t$ values for 0.5 probability level and 83 degrees of freedom as obtained from statistical table (Volk, 1958) is 1.96. Therefore 95% confidence ranging on the regression coefficients are

$$(b_1) = b_1 \pm 1.96\sqrt{s^2(b_1)} = 0.182925 \pm 0.1810747, \tag{40}$$

$$(b_2) = b_2 \pm 1.96\sqrt{s^2(b_2)} = 0.100930 \pm 0.0999098, \tag{41}$$

$$(b_3) = b_3 \pm 1.96\sqrt{s^2(b_3)} = -0.413661 \pm 0.4094819. \tag{42}$$

### 5.2. Significance of the correlation by F test

For checking the significance of the correlation the null hypothesis is used, i.e., it is assumed that the correlation is not significant. The $F$ value for the regression equation is,

$$F = 656.97. \tag{43}$$

The value for 83 degrees of freedom at 0.01 probability level obtained from statistical table (Volk, 1958) is

$$F_{0.01}(3, 111) = 3.74. \tag{44}$$

Since $F_{0.01}(3, 111) < F$, the null hypothesis may be rejected and it may be concluded that the correlation 4.36 is highly significant at 99.5% confidence level.

## 6. Conclusions

In the present investigation, a hydrocyclone was designed and fabricated. The system is designed in such a manner that it can operate in a wide range of variables for sand, sand–ash and sand–FCC system. In the present investigation a detailed study of performance of hydrocyclone, pressure drop, cut size particle diameter, and particle characterization has been carried out for the design and characterization of the hydrocyclone. A mathematical model for predicting particle separation efficiency and cut size particle diameter has been developed. A correlation has been developed for percentage removal of particles and retention of particles in the

hydrocyclone. The correlation has been statistically tested. Experimental findings for cut size particle diameter have been compared with the predictions made from the model as well as from other correlations available in the literature.

Experimental results and analysis reveal that this equipment is capable of separation of particles in the range of 75 μm. The present system can be used for particles above 175 μm with almost 100% particle separation efficiency. It gave very little separation for particles in the range below 60 μm which indicates that the experimental setup should be modified to increase separation efficiency for particles in the range of 10–50 μm. Various attempts have been made to modify the internals for improved efficiencies. However, due to shortage of time complete modifications have to be carried out in future study.

## Notation

| | |
|---|---|
| $a$ | diameter of air core in cyclone, m |
| $C_1$ | concentration of solid in suspension, kg/m$^3$ |
| $d$ | diameter of a particle, μm |
| $d_{50}$ | cut size diameter of particle, μm |
| $D_i$ | inlet diameter of hydrocyclone, m |
| $D_c$ | diameter of the hydrocyclone, m |
| $D_e$ | inside diameter of vortex finder or eductor, m |
| $D_u$ | underflow or spigot diameter, m |
| $f_2$ | function of variables |
| $g$ | acceleration due to gravity, m/s$^2$ |
| $L$ | total length of cyclone from top plate to apex, m |
| $Q$ | cyclone volume throughput, m$^3$/s |
| $R$ | radius of the hydrocyclone, m |
| $R_1$ | $R - \frac{1}{2}a - \frac{1}{2}D_i$ |
| RP | retention of particles in the hydrocyclone |
| $r$ | at any radius, m |
| $S$ | regression constant used in Eq. (25) |
| $U$ | radial velocity of liquid, m/s |
| $U_p$ | radial velocity of particle relative to the liquid, m/s |
| $V$ | Inlet velocity of fluid, m/s |
| $V_1$ | tangential velocity in cyclone, m/s |
| $W$ | axial velocity in cyclone, m/s |
| $Z$ | regression constant used in Eq. (24) |

*Greek letters*

| | |
|---|---|
| $\Delta\rho$ | difference between density of solid and that of liquid, kg/m$^3$ |
| $\Delta P$ | pressure drop across the hydrocyclone, N/m$^2$ |
| $\eta$ | particle efficiency of separation, % |
| $\mu_f$ | viscosity of fluid, N/m$^2$/s |
| $\rho$ | density of liquid, kg/m$^3$ |
| $\rho_s$ | density of suspended particle, kg/m$^3$ |
| $\phi$ | volumetric fraction of solids in the feed slurry |


## Acknowledgements

The authors thank the Chemical Engineering Department of IIT Kharagpur for extending the laboratory facilities to conduct part of the research work, and Mr. H. Jena of the Chemical Engineering Department, NIT Rourkela for helping with part of the computational analysis.


## References


Adupeasah, S.P., Diosady, L.L., Rubin, L.J., 1993. A multistage hydrocyclone stirred-tank system for countercurrent extraction of canola oil. Journal of American Oil Chemists Society 70, 755–762.

Bendixen, B., Rickwood, D., 1994. Effects of hydro-cyclones on the integrity of animal and microbial cells. Bioseparation 4.

Bradley, D., Pulling, D.J., 1959. Flow patterns in the hydraulic cyclone and their interpretation in terms of performance. Transactions of the Institute of Chemical Engineers 37, 34–45.

Chu, L.-y., Chen, W.-M., 1993. Research on the motion of solid particles in the hydro-cyclone. Separation Science and Technology 28, 1875–1886.

Chu, L.-y., Chen, W.-M., Lee, X.-Z., 2000. Effect of structural modification on hydro-cyclone performance. Separation and Purification Technology 21 (1–2), 71–86.

Chu, L.-y., Chen, W.-M., Lee, X.-Z., 2002a. Effects of geometric and operating parameters and feed characters on the motion of solid particles in hydro-cyclones. Separation and Purification Technology 26, 237–246.

Chu, L.-y., Chen, W.-M., Lee, X.-Z., 2002b. Enhancement of hydro-cyclone performance by controlling the inside turbulence structure. Chemical Engineering Science 57, 207–212.

Chu, L.-Y., Lee, X.-Z., Chen, W.-M., 1996. Energy consumption and its reduction in hydrocyclone separation process. Part I: Theoretical investigations of pressure distribution and energy consumption mechanism in hydrocyclones. In: Proceedings of the Seventh World Filtration Congress, Vol. 1, Budapest, Hungary, pp. 152–156.

Dahlstrom, D.A., 1951. Fundamentals and applications of the liquid cyclone. Chemical Engineering Progress Symposium Series No. 15; Mineral Engineering Techniques 50, 41–56.

Dhamo, N., 1994. An electrochemical hydro-cyclone cell for the treatment of dilute solutions-approximate plug-flow model for electrodeposition kinetics. Journal of Applied Electrochemistry 24, 745–750.

Dhamo, N., 1996. Electrochemical oxidation of cyanide in the hydro-cyclone cell. Waste Management 16, 257–261.

Dickey, L.C., daliner, M.F., Radewonuk, E.R., Parris, N., Kurantz, M., Craig, J.C., 1997. Hydro-cyclone separation of dry-milled corn. Cereal Chemistry 74, 676–680.

Dwari, R.K., 2003. Studies on the performance characteristics of a hydrocyclone separator. M. Tech Dissertation, National Institute of Technology, Rourkela.

Fahlstorm, P.H., 1963. Studies of the hydro-cyclone as classifier. Mineral processing, Proceedings of the Sixth International Congress, Cannes.

Heish, K.T., Rajamani, R.K., 1991. Mathematical model of the hydro-cyclone based on physics of fluid flow. American Institute of Chemical Engineers Journal 37 (5), 735–746.

Kelsall, D.F., 1952. A study of the motion of solid particles in a hydraulic cyclone. Trans Institute of Chemical Engineers 30, 87–107.

Klima, M.N., Kim, B.H., 1997. Multi-stage wide-angle hydro-cyclone circuits for removing fine, high density particles from a low density soil matrix. Journal of Environmental Science and Health 32, 715–733.

Klima, M.N., Kim, B.H., 1998. Dense-medium separation of heavy-metal particles from soil using awide-angle hydro-cyclone. Journal of Environmental Science and Health 33, 1325–1340.

Larson, T., 1980. A new type of hydro-cyclone. Proceedings of the First International Conference on Hydro-cyclones, Cambridge, UK.

Li, M., Johnston, L., Xu, L., Filonko, Y., Parker, I., 1999. Characterization of hydro-cyclone-separated eucalypt fiber fractions. Journal of Pulp Paper and Science 25 299–304.

Lin, I.J., 1987. Hydro-cyclone thickening; dewatering and densification of fine particulates. Separation Science and Technology 22, 1327–1347.

Luo, Q., Deng, C.L., Xu, L.X., Yu, L., Xiong, G.A., 1989. Comparison of the performance of water-sealed and commercial hydro-cyclones. International Journal of Mineral Processing 25, 297–310.

Lynch, A.J., Rao, T.C., 1966. Studies on the operating characteristics of hydro-cyclone classifiers. Indian Journal of Technology 6, 106–114.

Lynch, A.J., Rao, T.C., 1975. Modeling and scale-up of hydro-cyclone classifier. Eleventh International Mineral Processing Congress, Cagliari.

Meikap, B.C., Kundu, G., Biswas, M.N., 2002. Scrubbing of Fly ash laden $SO_2$ in a multi-stage bubble column scrubber. American Institute of Chemical Engineers Journal 48 (8), 2074–2083.

Peachey, B.R., Solanki, S.C., Zahacy, T.A., Piers, K., 1998. Downhole oil/water separation moves into high gear. Journal of Canadian Petroleum Technology 37, 34–41.

Rietima, K., 1961. Performance and Design of Hydro-cyclone-I, II, III, IV. Chemical Engineering Science 15, 298–325.

Singh, N., Eckhoff, S.R., 1995. Hydrocyclone procedure for starch-protein separation in laboratory wet-milling. Cereal Chemistry 72, 344–348.

Trim, D.S., Marder, R.C., 1995. Investigation of hydro-cyclones for concentration of cassava milk. Starch-Strake 47, 344–348.

Yuan, H., Richwood, D., Smyth, I.C., Thew, M.T., 1969. An investigation into the possible use of hydro-cyclones for the removal of yeast from beer. Bioseparation 6, 159–163.